Journal of Advanced Research in Applied Sciences and Engineering Technology

Journal homepage:
https://semarakilmu.com.my/journals/index.php/applied_sciences_eng_tech/index
ISSN: 2462-1943

Formulation of Catalytic Deep Eutectic Solvent for H_2S Oxidative Absorption at Ambient Condition with Assistance of Cosmo-Rs

Nor Fariza Abd Mutalib[1,*], Muhammad Shazwan Shabani[1], Mohamad Azmi Bustam[1]

[1] Department of Chemical Engineering, Universiti Teknologi PETRONAS, 32610 Seri Iskandar, Perak, Malaysia

ARTICLE INFO

Article history:
Received 23 August 2023
Received in revised form 31 December 2023
Accepted 18 January 2024
Available online 7 February 2024

Keywords:
Catalytic Deep Eutectic Solvent; Direct conversion; Hydrogen sulfide; Sulfur; Transition metal

ABSTRACT

H_2S is very well known for its toxicity, corrosivity, flammability and explosiveness which in overall lead to operational difficulty. Hence, raising the need for H_2S sweetening process. However, the current conventional sweetening process is very energy intensive besides suffer from catalyst deactivation issue. Therefore, raising the need for more environmentally and economical friendly approach such as utilizing green solvent like deep eutectic solvent. Thus, the objective of this research is to determine the best combination of HBD and HBA components for catalytic DESs to convert H_2S at room temperature. The study utilized COSMO-RS computational to assist in selecting the appropriate components, synthesized and characterized the chosen catalytic DES, and performed oxidative absorption of H_2S using the selected DES. Initially, the solubility and selectivity performance of various HBD and HBA were evaluated, and the components with the best performance were combined with $CuCl_2.2H_2O$ to form catalytic DES. The synthesized catalytic DES was characterized using FTIR and tested for its oxidation absorption capability. Based on the COSMO-RS screening, 1-butyl-3-methylimidazoilum chloride [bmim][Cl] and ethylene glycol [EG] were determined to be the best HBD and HBA, respectively. The catalytic DES formed from these components was homogeneous and brown in colour. The results of oxidative absorption showed that the catalytic DES rapidly produced a yellow precipitate, which was later confirmed to be sulphur. The study concludes that COSMO-RS computational can be used to formulate DESs for H_2S oxidative absorption, and catalytic DES maintained its properties before and after H_2S oxidation. The research also suggests that oxidative absorption of H_2S to sulphur using catalytic DESs is a feasible and rapid.

1. Introduction

In the coming years, it is anticipated that the usage of fossil fuels will vary significantly as more organizations adopt sustainable and environmentally friendly solutions [1]. Wang *et al.,* [2] has reported that in the BRICS Energy Report as shown in Figure 1, that the use of fossil fuel particularly coal and oil, is expected to decrease overall [1]. However, natural gas is expected to grow due to its relatively smaller carbon footprint compared to other fossil fuels [3]. This trend has led to the

* *Corresponding author.*
E-mail address: nor_20002068@utp.edu.my

https://doi.org/10.37934/araset.39.1.192205

development of solutions that are both environmentally friendly and viable for industrial use. Despite the advantages of natural gas, its production still faces hurdles, particularly in the production of gas contaminant such as hydrogen sulphide (H_2S). Natural gas is considered sour when the H_2S gas is approximately more than 4 ppm by volume under standard temperature and pressure [4]. It presents major problem due to its high toxicity, flammability, explosivity and corrosivity [5-9]. Therefore, it is very important to remove H_2S from the gas stream or alternatively, converting it into a lesser hazardous and more valuable material such as elemental sulfur. H_2S conversion benefits not only for downstream operation but for environmental protection and human health.

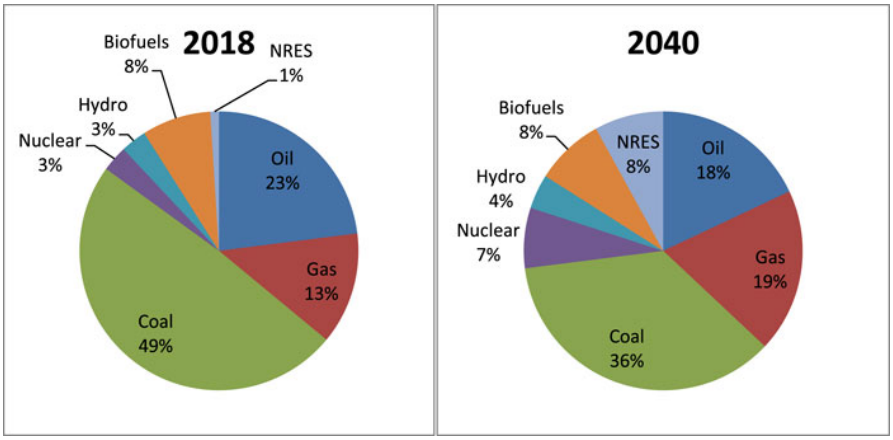

Fig. 1. Depicts the Energy Consumption Trends in The BRICS Energy Report For 2018 and the Predicted Trends For 2040 [1]

Sweetening process is used to remove H_2S gas to an allowable level [10,11]. The removed H_2S gas is then sent to a processing plant or a Sulfur Recovery Unit (SRU) where it is converted into solid sulphur [12,13]. Recently, the sulphur extracted has a commercial value of approximately 240 USD/kg as of 2019 making it a profitable side business, as it has many applications ranging from water processing to the production of sulphur-based fertilizers [14]. Both processing plants and SRUs use the Claus process to convert H_2S into sulphur which is the most popular method. The Claus process is a catalytic two-step process that is conducted at a very high temperatures for the reaction to occur [10]. Besides, this high temperature requirement is also to avoid sulfur condensation on the catalyst surface [15]. However, such temperature condition is not beneficial to the conversion of H_2S since the reaction is highly exothermic. Besides, there are some other drawback associates with this technology, for instances, this technology suffers from intensive energy usage and SO_2 gas released to the atmosphere during acid gas flaring which pollute the environment [16]. Hence, a more environmentally and economical friendly approach is required for H_2S removal.

Such approach can be obtained by utilizing green solvent which quite recently, green solvents like ionic liquid (ILs) and deep eutectic solvents (DESs) have gained the interest of researchers due to their versatile properties. ILs are highly polar, non-volatile, chemically inert, and have good solubility with organic and inorganic materials, and are well known for its task specific tuning properties making it an excellent fit for a green solvent for gas separation process [17-22]. Owing to its specific tuning properties that enable development of green solvents with unique combination of properties for targeted application, catalytic ILs which consist of transition metal coupled to either anion and/or cation, are introduced [23]. The presence of transition metal gives some advantages such as ILs can exist in many oxidations state due to the incomplete d-orbital. Therefore, making it suitable for oxidation and reduction processes.

Huang *et al.,* [24] in their study found that [bmim][$FeCl_4$] are highly efficient in capturing and converting H_2S. Not only that, it also gives impressive one-stage conversion ratio of more than 99% [25]. Li *et al.,* [26] in another study reported H_2S oxidation efficiency of $Et_3NHCl \cdot FeCl_3$ that reached up to 87.9%. Despite catalytic ILs proven massive performance in converting H_2S to elemental sulfur, to our knowledge, study of catalytic DESs is still rare. Similar to ILs, DESs also has high thermal stability, low volatility and highly tuneable. The only difference from ILs is the structure of DESs which it is structured by hydrogen bonding between the hydrogen bond donor (HBD) and hydrogen bond acceptor (HBA). This result in lower melting point as they have lower anion and cation interaction [27]. This benefits DESs as it will have wider range of appearing in liquid form which favoured process which is design to operate at ambient condition. To date, only Lin *et al.,* [28] reported H_2S oxidized to sulfur rapidly by Fe-based DESs to be specific (ChCl)/glycol. Providing huge potential for exploration of catalytic DESs, just like ILs, there are also massive possible combination of hydrogen bond donor and hydrogen bond acceptor to form DESs. Exploring their potential via trial-and-error method would be waste of resources, time and cost. This study aims to provide insights into the optimal formulation of DESs for H_2S conversion by selecting suitable HBD and HBA components. However, a comprehensive analysis of DESs ability to convert H_2S compared to established methods is beyond the scope of this study and may be addressed in future research. The paper commences with an examination of the materials used and subsequently details the methodology employed to identify the ideal HBA and HBD components for DESs synthesis for H_2S conversion.

2. Methodology

2.1 Materials

1-butyl-3-methylimidazolium chloride [bmim][Cl], (98% purity) was purchased from AcrosOrganics. Copper (II) Chloride dihydrate ($CuCl_2.2H_2O$), ACS reagent (≥99% purity) was purchased from Sigma Aldrich. Ethylene glycol [EG] anhydrous, (99.8% purity) was purchased from Sigma Aldrich. All chemicals are used as received without further purification. Other chemical like sodium hydroxide (≥97%) pellets for analysis was purchase from Merck.

2.2 Computational Modelling using COSMO-RS

Mutalib *et al.,* [29] suggest that in order for a reaction to be effective in a liquid medium, it is important for the solute to be sufficiently soluble in the solvent. This is because when solutes are well-dissolved in a solution, it allows for the free movement of reactants throughout the liquid, leading to a more homogeneous interaction of reactants [21]. Therefore, it can be inferred that solubility plays a critical role in conversion, and any parameters that affect solubility will also have a direct impact on conversion efficiency thus it is essential that the synthesize deep eutectic solvent (DESs) to have high solubility towards H_2S gas. However, since DESs are composed of hydrogen bond donors (HBD) and acceptors (HBA), there are numerous possible combinations, which would be time-consuming to investigate experimentally. To overcome this challenge, a computational platform, COSMO-RS, is being utilized to predict the solubility of H_2S in HBD and HBA, so that the combination with the highest solubility can be selected to form a DES.

In addition to solubility, selectivity is also a significant parameter to consider. This is particularly relevant because gas mixtures often consist of multiple components. For instance, acid gases are typically composed of higher concentrations of CO_2 than H_2S. As such, it is essential to predict the selectivity value of HBD and HBA towards H_2S relative to CO_2 in this study, given its practical implications.

2.2.1 Screening of HBDs and HBAs

In this study, the selection of HBD was limited to imidazolium-based compounds for several reasons. Firstly, their synthesis route is straightforward, and they are readily available at a reasonable cost [30]. Secondly, they have been found to possess high thermal stability [31]. The chosen HBDs were selected from the available COSMOtherm database and were analysed at a single conformer with the least ground-state energy, using the TZVP basis set for computation purposes.

Using COSMO-RS, the solubility of the HBDs was subsequently forecasted at a pressure of 1 bar, and this was achieved by utilizing the following Eq. (1) as calculated by COSMO-RS [32].

$$p_{H_2S} = p^0_{H_2S} \cdot x_{H_2S} \cdot \gamma_{H_2S} \tag{1}$$

The solubility calculations involved taking into account the partial pressure of H_2S (p_{H2S}), as well as the vapor pressure of pure H_2S (p^0_{H2S}), alongside the mole fraction, (x_{H2S}) and activity coefficient (γ_{H2S}) of H_2S [32]. The resulting solubility values were then reported in terms of the H_2S mole fraction present in the liquid phase.

In the meantime, selectivity was determined through the computation of the activity coefficient at infinite dilution, using the following Eq. (2) [33]:

$$S^{\infty} = \frac{\gamma^{\infty}_{CO_2}}{\gamma^{\infty}_{H_2S}} \tag{2}$$

where γ^{∞}_{CO2} and γ^{∞}_{H2S} are the activity coefficients for CO_2 and H_2S at infinite dilution, respectively. The process of screening the HBA was akin to the aforementioned approach. The HBAs examined in this study consisted of ethylene glycol, glycerol, and urea.

In order to gain a deeper understanding of the investigated molecules behaviour, the sigma profile and sigma potential were analysed. A thorough understanding of the behaviour and interaction of molecules is essential for the effective selection of task specific DESs. The equations utilized for the calculation of both the sigma profile and sigma potential are presented in Eq. (3) and Eq. (4), respectively [32]:

$$p^{Xi} = \frac{n_i(\sigma)}{n_i} = \frac{A_i(\sigma)}{A_i} \tag{3}$$

$$\mu_s(\sigma) = -\frac{RT}{\alpha_{eff}} \ln\left[\int p_s(\sigma') \exp\left(\frac{\alpha_{eff}}{RT}\left(\mu_s(\sigma') - e(\sigma - \sigma')\right)\right) d\sigma'\right] \tag{4}$$

For Eq. (3), $p^{Xi}(\sigma)$ is the sigma profile of any molecule X, $n_i(\sigma)$ is the number of distributed segments that has surface charge density σ, n_i is the total number of distributed segments, $A_i(\sigma)$ is the segment surface area that has surface charge density σ, A_i is the area of the whole surface cavity rooted in the medium and σ is the polarity of the surface. Meanwhile, for Eq. (4), $\mu_s(\sigma)$ is the chemical potential of a surface segment, R is the universal gas constant, T is the temperature at which the vapor pressure is estimated, α_{eff} is the chemical potential of an effective surface segment of

area, $p_s(\sigma')$ is the sigma profile of the whole system and $\mu_s(\sigma')$ is the chemical potential of a surface segment.

In general, to select the most suitable HBA and HBD, the solubility and selectivity values were considered. Furthermore, the sigma profile and sigma potential were utilized to examine and elucidate the characteristics of the HBA and HBD molecules.

2.3 Synthesize of DES-CuCl.2H_2O

An equimolar amount of EG was mixed with [bmim]Cl and stirred continuously at 180 rpm for 24 hours. After that, $CuCl_2.H_2O$ was added to the resulting DES solution and stirred continuously at 180 rpm for another 24 hours. The DES-$CuCl_2.H_2O$ solutions were synthesized equimolar amount of $CuCl_2.H_2O$ to DES solution.

2.4 Fourier Transform Infrared Spectroscopy (FTIR) Analysis for DES-CuCl.2H_2O

[bmim][Cl], EG and [bmim][Cl]-EG solution (DES) were first evaluated by using FTIR. This was to confirm that the [bmim][Cl] and EG only physically mixed and not chemically react in order to form the DES [bmim][Cl]-EG. Next, the $CuCl_2.2H_2O$ and the mixture of DES- $CuCl_2.2H_2O$ were evaluated. The evaluation was done by mean of Attenuated Total Reflection (ATR) method using on Thermo Scientific FTIR- model Nicolet iS5 at room temperature and interpreted by using OMNIC software.

2.5 Raman Spectroscopy

uRaman Microscopy Module model uRaman-532TEC-LV (532nm) was used with the assistance of uSOFT software. The amplification of objective lens is 20 times. The acquisition time was set to 1000 ms and average of 10. Also, the laser power was kept at 75 W. The spectrum was then collected and compared with the data available in the literature.

2.6 H_2S Oxidative Absorption

The apparatus set-up for the absorption and oxidation of H_2S DES-$CuCl_2.2H_2O$ was shown in Figure 2. H_2S from the tank was first bubbled through a predetermined amount of DES (3.5 ml) loaded in the reactor cell at a flow rate of 16 mL/min. At 20 minutes, the reactor tube was weighed using a balance to obtain the mass of sulphur produced, which was equivalent to the mass of H_2S oxidized. The off H_2S gas was treated with a scrubber containing a 1M NaOH solution to reduce it to a safer level below 3ppm.

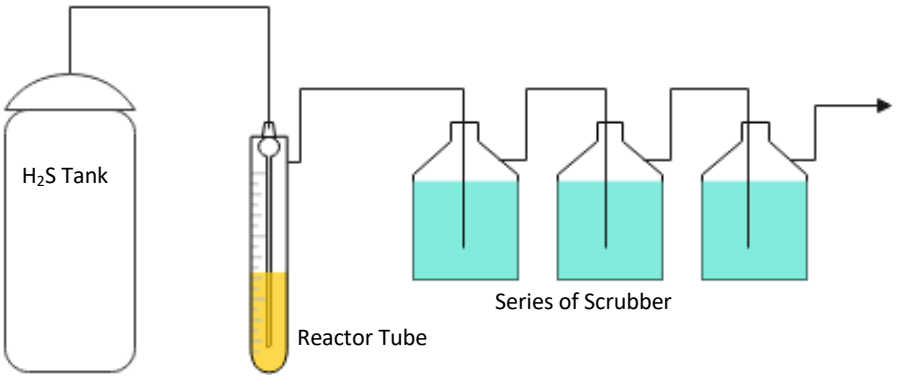

Fig. 2. Oxidative absorption experimental setup

3. Results

3.1 COSMO-RS Hydrogen Bond Donor Screening and Selection

The solubility values of H_2S in the HBD were presented in the table below. According to the Table 1, the solubility followed the order [emim][Cl] > [bmim][Cl] > [hmim][Cl]. This trend contradicts the claim made by Aki *et al.,* [34] in their study, where they suggested that the solubility increases with longer alkyl chain length due to a decrease in molar density, as found by Fredlake *et al.,* [35]. This finding was also supported by Gu and Brennecke [36] who found that compounds with longer alkyl chain lengths have a larger molar volume. However, the results of this study revealed that considering molar volume alone is not sufficient to explain the overall behaviour of H_2S solubility. This claim was further supported by Sakhaeinia *et al.,* [37] who found that the molar volume of [emim][$EtSO_4$] was higher than [emim][Tf_2N] and [HOemim][Tf_2N] and lower than [HOemim][PF_6], [HOemim][BF_4], [emim][PF_6] and [emim][BF_4]. However, the H_2S solubility in [emim][$EtSO_4$] was the lowest. Therefore, important to note that the anion plays a crucial role in H_2S solubility in the HBD, primarily due to its good hydrogen bond acceptor character. The solubility result can be further explained by analysing the sigma profile and sigma potential of H_2S in the HBD, as shown in Figure 3 and Figure 4, respectively.

Table 1
COSMO-RS predicted H_2S solubility and selectivity value of the HBDs

Hydrogen Bond Donor	Solubility (mol H_2S/mol HBD)	Selectivity
[emim][Cl]	0.6530	0.7433
[bmim][Cl]	0.6457	1.1761
[hmim][Cl]	0.6411	1.3554

The sigma profile of H_2S and imidazole based HBD was presented in Figure 3 and was categorized into three regions: the hydrogen bond donor region, which covers a polarity range of $\alpha < -0.0082$ e/Å^2, the hydrogen bond acceptor region, which covers a polarity range of $\alpha > +0.0082$ e/Å^2, and the non-polar region, which covers a polarity range of -0.0082 e/Å$^2 < \alpha < 0.0082$ e/Å^2 [38]. The profile of H_2S shows two distinct peaks in the range of +0.005 to -0.01 e/Å$_2$, indicating that it has both non-polar and hydrogen bond donor properties. However, the non-polar properties appear to be more dominant due to the stronger peak in the non-polar region, meaning H_2S better interact with HBD with non-polar properties.

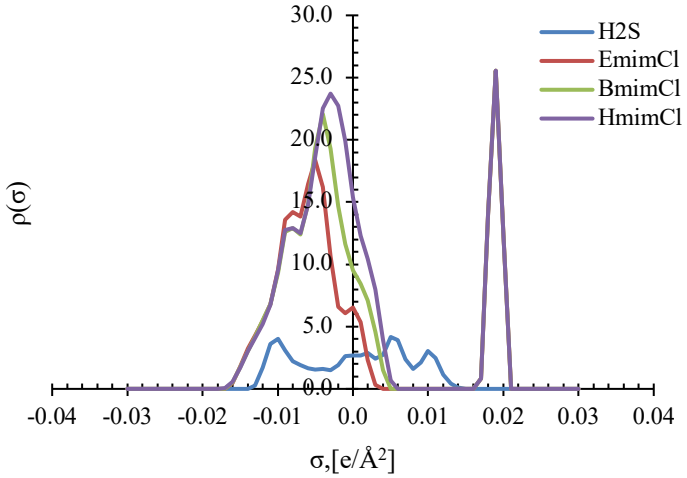

Fig. 3. Sigma potential of the H_2S and HBDs

Furthermore, it was observed that all three cations have similar trends, the only difference is their degree of spread. The difference in spreading talks about the polarity strength meaning the more spread out, the more polar is the cation. However, since our H_2S is dominated by non-polar properties, meaning it will react better with HBD that has good non-polar properties which in this case, HBD with cation that is more centered (less spread out). Therefore, from the profile, it says that [emim][Cl] is the best HBD followed by [bmim][Cl] and [hmim][Cl]. This finding was in an agreement with the sigma potential in Figure 4 where [emim][Cl] has the most negative value in the hydrogen bond donor and non-polar region meaning it has the highest affinity towards H_2S which is both hydrogen bond donor and non-polar. However, from Table 1, even though [emim][Cl] has the highest H_2S solubility, its selectivity towards H_2S is the lowest. From a practical point of view, this is concerning because this tells that [emim][Cl] has higher tendency of absorbing other gases like CO_2 instead of H_2S. Therefore, considering both solubility and selectivity element, [bmim][Cl] was decided as the best HBD.

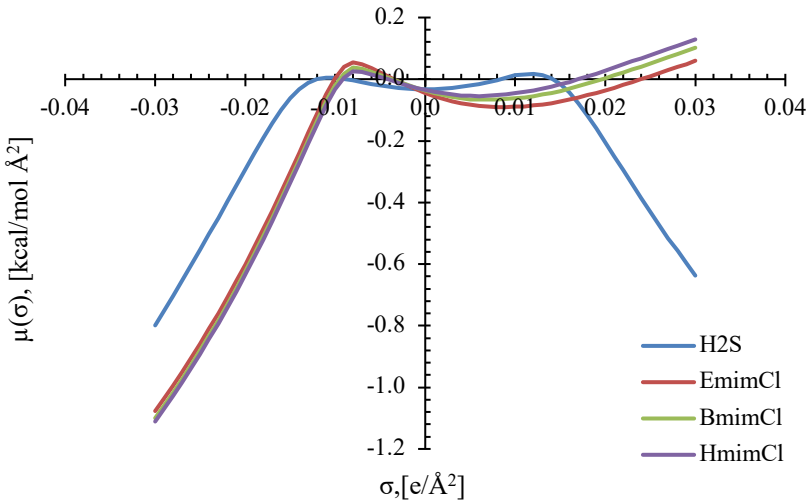

Fig. 4. Sigma potential of the H_2S and HBDs

3.2 COSMO-RS Hydrogen Bond Acceptor Screening and Selection

The following Table 2 provides information on the solubility and selectivity values of the HBAs. Generally, it can be observed that ethylene glycol has the highest solubility followed by glycerol and

then urea. On the other hand, the order of selectivity is ethylene glycol > urea > glycerol. These results, like in the previous sub-section, can also be analysed through the sigma profile and sigma potential.

Table 2
COSMO-RS predicted H_2S solubility and selectivity value of the HBAs

Hydrogen Bond Acceptor	Solubility (mol H_2S/mol HBA)	Selectivity
Ethylene Glycol [EG]	0.2400	1.3350
Glycerol	0.1782	0.7560
Urea	0.1162	0.7610

The sigma potential graph shown in the Figure 5(a) below illustrates that both ethylene glycol (EG) and glycerol have a distinctive peak in the non-polar region, indicating that they are both non-polar. However, EG is more non-polar than glycerol in terms of intensity as it displays a more prominent peak than glycerol. This is why EG interacts more effectively with H_2S, following the principle of "like dissolves like." Meanwhile, urea displays a distinct peak in the hydrogen bond donor region, implying that it can interact with H_2S since H_2S also possesses hydrogen bond donor properties. Nonetheless, its interaction with H_2S is not as robust as that of EG and glycerol because the H_2S hydrogen bond donor properties are weaker compared to its non-polar properties. This outcome is supported by the sigma potential graph in Figure 5(b), which reveals that EG has the lowest negative value in the non-polar region, followed by glycerol and urea. This suggests that EG has a stronger inclination towards non-polar compounds such as H_2S.

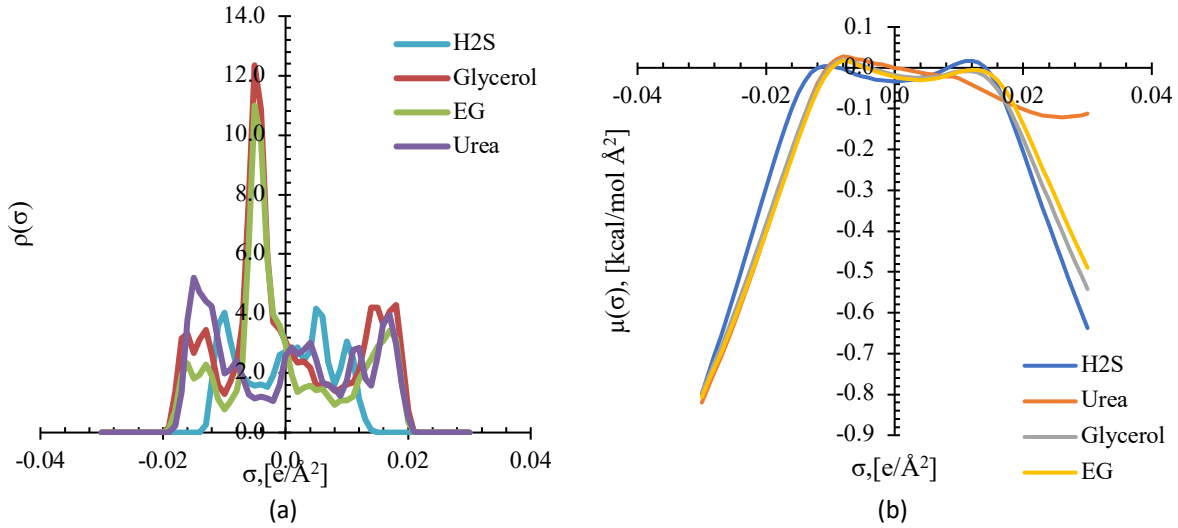

Fig. 5. (a) Left: Sigma profile of the H_2S and HBAs (b) Right: Sigma potential of the H_2S and HBAs

3.3 Formation of Catalytic DESs [bmim][Cl]/EG - $CuCl_2.2H_2O$

According to the results obtained in the previous section, DES is formed by combining [bmim][Cl] and EG. This DES is then mixed with $CuCl_2.2H_2O$ to create a catalytic DES. $CuCl_2.2H_2O$ is chosen because, like $FeCl_3$, it is inexpensive and easily accessible [39]. Additionally, it is a highly effective Lewis acid catalyst [40].

Figure 6 shown below depicts the visual characteristics of the DES and the catalytic DES. Both the DES and catalytic DES have a homogeneous appearance. The color of the homogeneous DES changes from light yellow to brown upon the addition of $CuCl_2.2H_2O$. The homogeneous state provides

significant benefits in terms of mass transfer, making it more suitable for milder conditions such as ambient conditions [14].

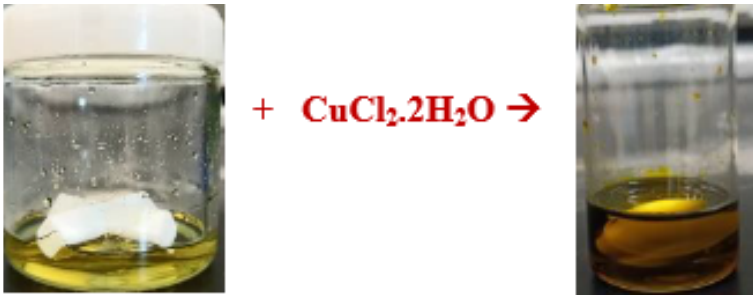

Fig. 6. Formation of Catalytic DESs [bmim][Cl]/EG - $CuCl_2.2H_2O$

3.4 FTIR Identification

The Figure 7(i) presented below shows the FTIR spectrum of [bmim][Cl], EG, and DES [bmim][Cl]/EG. Figure 7(i)(c) indicates that the DES spectrum is an overlap of the [bmim][Cl] and EG spectra, suggesting that the DES is formed through physical mixing only. In Figure 7(i)(a), the appearance of the -OH band at ~3774 cm^{-1} is evident, and the peaks within ~2873 and ~2960 cm^{-1} are attributed to the stretching vibrational behaviour of (-C-H), ($-CH_2$), and ($-CH_3$) of the alkyl functional groups that are connected to the nitrogen atoms in the imidazolium ring of the HBD [41,42]. Peaks between ~2960 and ~3147 cm^{-1} are assigned to the stretching behaviour of the (-CH) bond belonging to $[bmim]^+$. The peaks observed within ~1563 and ~1462 cm^{-1} are attributed to the complete structural behaviour of the imidazolium ring [42].

Peaks between ~2960 and ~3147 cm^{-1} are assigned to the stretching behaviour of the (-CH) bond belonging to $[bmim]^+$. The peaks observed within ~1563 and ~1462 cm^{-1} are attributed to the complete structural behaviour of the imidazolium ring [42]. In Figure 7(i)(b), the peak at 3284.55 cm^{-1} indicates the O-H bond, while the peaks at 1082 cm^{-1} and 1031 cm^{-1} indicate the O-H bond and C-O-H bond present in EG. The peaks observed at the wavenumber of 3340 cm^{-1} and 1575 cm^{-1} in Figure 7(ii)(a) indicate the O-H bond, and the characteristic peak for Cu-Cl bond is observed at 1129 cm^{-1}. The catalytic DES in Figure 7(ii)(b) also consists of overlapping peaks between $CuCl_2.2H_2O$ and DES only, with no new peaks formation or peaks disappearance observed in the resulting DES-$CuCl_2.2H_2O$ mixture FTIR spectra, confirming the successful synthesis of the DES-$CuCl_2.2H_2O$ mixture.

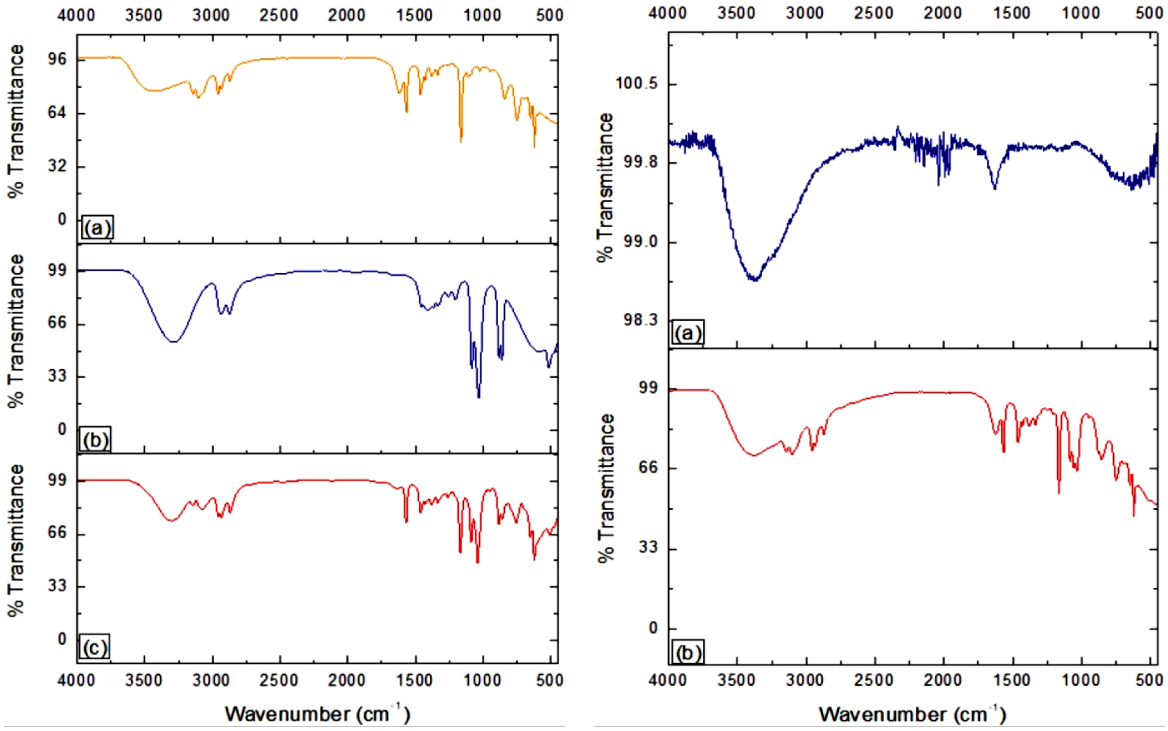

Fig. 7. (i) FTIR spectra of [bmim][Cl], EG and DES (ii) FTIR spectra of $CuCl_2.2H_2O$ and DES- $CuCl_2.2H_2O$

3.5 Oxidative Oxidation

The aim of this study was to investigate the use of catalytic DES for the oxidative absorption of H_2S into elemental sulphur. Figure 8(b) shows that the colour of the sample remained unchanged throughout the oxidation process and yellow solid precipitates formed rapidly. The yellow precipitate was analysed using Raman spectra (refer Figure 8(a)) and significant peaks were observed at 153 cm^{-1}, 220 cm^{-1} and 473 cm^{-1}, while the remaining peaks at around 433, 245, and 191 cm^{-1} were minor peaks. The peak obtained from the solid precipitate was compared with the peak produced by octasulphur (S_8), and it was confirmed that the solid precipitate formed was sulphur [3,8,17]. The other peaks were attributed to the catalytic DES used in the process.

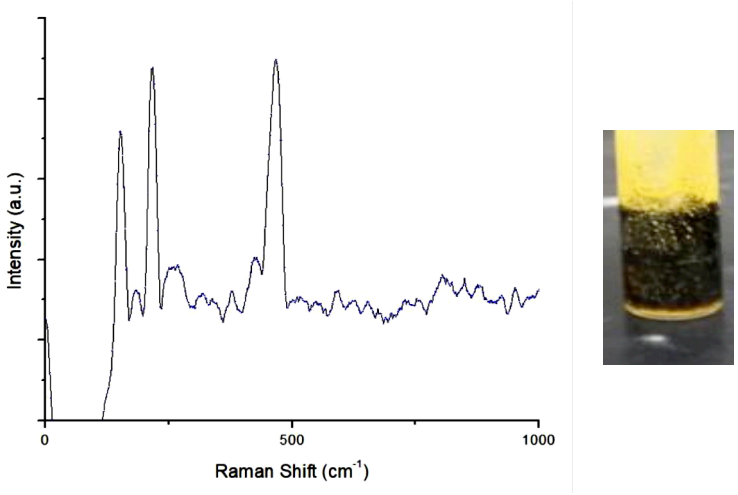

Fig. 8. (a) Raman spectra of spent DES- $CuCl_2.2H_2O$ (b) Spent DES- $CuCl_2.2H_2O$

The catalytic DES did not show any new peaks or disappearing peaks in the spent DES-$CuCl_2.2H_2O$ mixture (refer Figure 9), indicating that the mixture's structure remained unchanged even after the conversion reaction took place. This suggests that the DES solution itself was not directly involved in the reaction, but instead acted as a medium for H_2S absorption and dissolution to enable the conversion to occur. The characterization findings support the pre-conclusion that the oxidative absorption of H_2S to elemental sulphur follows the reaction shown below:

$$2[bmim][Cl]/[EG].CuCl_2.2H_2O + H_2S \rightarrow 2[bmim][Cl]/EG.CuCl_2H + 2H_2O + S$$

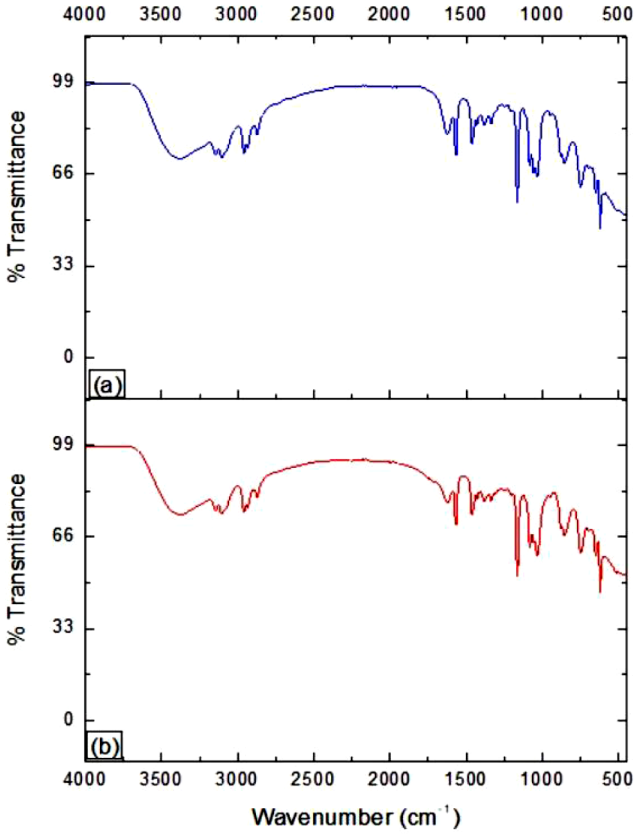

Fig. 9. FTIR of (a) pure DES- $CuCl_2.2H_2O$ (b) spent DES-$CuCl_2.2H_2O$

4. Conclusions

To summarize, this study aimed to determine the optimal formulation of DESs for H_2S conversion by screening various HBD and HBA components using COSMO-RS to assess their solubility. The results showed that [bmim][Cl] as the HBD and EG as the HBA had the best solubility and selectivity values. This was supported by the sigma potential and sigma profile analysis which demonstrated their excellent non-polar properties. These components were then combined with $CuCl_2.2H_2O$ to produce a brown homogenous catalytic DES through physical mixing. The study showed that H_2S was rapidly converted to sulphur when absorbed into the catalytic DES. Further research is needed to optimize parameters and conduct a more comprehensive qualitative and quantitative analysis to fully explore the potential of catalytic DES.

Acknowledgement

This research was funded by a grant from Yayasan Universiti Teknologi PETRONAS, grant number 015LCO-418.

References

[1] Osorio, Andre Luiz Rodrigues, Joao Antonio Moreira Patusco, Vyacheslav Kulagin, Dmitry Grushevenko, Nikita Kapustin, Xu Xiaodong, Gu Hongbin, He Zhao, and Yan Bingzhong. "BRICS. ENERGY REPORT 2020." *Ministry of Energy of the Russian Federation* (2020).

[2] Wang, Hong, Muhammad Asif Amjad, Noman Arshed, Abdullah Mohamed, Shamsher Ali, Muhammad Afaq Haider Jafri, and Yousaf Ali Khan. "Fossil energy demand and economic development in BRICS countries." *Frontiers in Energy Research* 10 (2022): 842793. https://doi.org/10.3389/fenrg.2022.842793

[3] Tinivella, Umberta, Michela Giustiniani, Ivan de la Cruz Vargas Cordero, and Atanas Vasilev. "Gas hydrate: environmental and climate impacts." *Geosciences* 9, no. 10 (2019): 443. https://doi.org/10.3390/geosciences9100443

[4] Koczo, Kalman, Mark D. Leatherman, and Jonathan J. Wylde. "Foam control." In *Surface Process, Transportation, and Storage*, pp. 153-226. Gulf Professional Publishing, 2023. https://doi.org/10.1016/B978-0-12-823891-2.00002-8

[5] Hantson, Ph, F. J. Baud, and R. Garnier. "Toxic gases." *Human Toxicology* (1996): 661-669. https://doi.org/10.1016/B978-044481557-6/50028-9

[6] Rahnama-Moghadam, Sahand, L. David Hillis, and Richard A. Lange. "Environmental toxins and the heart." In *Heart and Toxins*, pp. 75-132. Academic Press, 2015. https://doi.org/10.1016/B978-0-12-416595-3.00003-7

[7] Bai, Yong, and Qiang Bai. "Subsea corrosion and scale." *Subsea Engineering Handbook* (2019): 455-487. https://doi.org/10.1016/B978-0-12-812622-6.00017-8

[8] Selley, Richard C. *Elements of petroleum geology*. Gulf Professional Publishing, 1998.

[9] Mokhatab, Saeid, and William A. Poe. "Chapter 7-natural gas sweetening." *Handbook of Natural Gas Transmission and Processing* 2 (2012): 253-290. https://doi.org/10.1016/B978-0-12-386914-2.00007-8

[10] Stewart, Maurice. *Surface Production Operations: Vol 2: Design of Gas-Handling Systems and Facilities*. Vol. 2. Gulf Professional Publishing, 2014.

[11] Mokhatab, S., W. A. Poe, and J. Y. Mak. "Gas processing plant automation." *Handbook of Natural Gas Transmission and Processing; Elsevier: Amsterdam, The Netherlands* (2019): 615-642. https://doi.org/10.1016/B978-0-12-815817-3.00020-4

[12] Jafarinejad, Shahryar. "Control and treatment of sulfur compounds specially sulfur oxides (SOx) emissions from the petroleum industry: a review." *Chemistry International* 2, no. 4 (2016): 242-253.

[13] Wiheeb, Ahmed Daham, Ili Khairunnisa Shamsudin, Mohd Azmier Ahmad, Muhamad Nazri Murat, Jinsoo Kim, and Mohd Roslee Othman. "Present technologies for hydrogen sulfide removal from gaseous mixtures." *Reviews in Chemical Engineering* 29, no. 6 (2013): 449-470. https://doi.org/10.1515/revce-2013-0017

[14] Wang, Lan-yun, Yong-liang Xu, Zhen-dong Li, Ya-nan Wei, and Jian-ping Wei. "CO_2/CH_4 and H_2S/CO_2 selectivity by ionic liquids in natural gas sweetening." *Energy & Fuels* 32, no. 1 (2018): 10-23. https://doi.org/10.1021/acs.energyfuels.7b02852

[15] Kohl, A. L., and R. B. Nielsen. "Chapter 8 Sulfur Recovery Processes." *Gas Purification* (1997): 670-730. https://doi.org/10.1016/B978-088415220-0/50008-2

[16] Al-shafei, Mansour A. "Manufacture of Portland cement using spent claus catalyst." *U.S. Patent 8,029,618*, issued October 4, 2011.

[17] Zhao, Qichao, and Jared L. Anderson. "Task-specific microextractions using ionic liquids." *Analytical and Bioanalytical Chemistry* 400 (2011): 1613-1618. https://doi.org/10.1007/s00216-011-4848-z

[18] Dharaskar, Swapnil A., Kailas L. Wasewar, Mahesh N. Varma, Diwakar Z. Shende, and Chang Kyoo Yoo. "Ionic liquids:-the novel solvent for removal of dibenzothiophene from liquid fuel." *Procedia Engineering* 51 (2013): 314-317. https://doi.org/10.1016/j.proeng.2013.01.042

[19] Karuppasamy, K., Jayaraman Theerthagiri, Dhanasekaran Vikraman, Chang-Joo Yim, Sajjad Hussain, Ramakant Sharma, Thandavaryan Maiyalagan, Jiaqian Qin, and Hyun-Seok Kim. "Ionic liquid-based electrolytes for energy storage devices: A brief review on their limits and applications." *Polymers* 12, no. 4 (2020): 918. https://doi.org/10.3390/polym12040918

[20] Paulechka, Y. U., Dz H. Zaitsau, G. J. Kabo, and A. A. Strechan. "Vapor pressure and thermal stability of ionic liquid 1-butyl-3-methylimidazolium Bis (trifluoromethylsulfonyl) amide." *Thermochimica Acta* 439, no. 1-2 (2005): 158-160. https://doi.org/10.1016/j.tca.2005.08.035

[21] Ratti, Rajni. "Ionic liquids: synthesis and applications in catalysis." *Advances in Chemistry* 2014, no. 3 (2014): 1-16. https://doi.org/10.1155/2014/729842

[22] Sawant, A. D., D. G. Raut, N. B. Darvatkar, and M. M. Salunkhe. "Recent developments of task-specific ionic liquids in organic synthesis." *Green Chemistry Letters and Reviews* 4, no. 1 (2011): 41-54. https://doi.org/10.1080/17518253.2010.500622

[23] Lang, Kwong Cheng, Lian See Tan, Jully Tan, Azmi Mohd Shariff, and Hairul Nazirah Abdul Halim. "Life cycle assessment of potassium lysinate for biogas upgrading." *Progress in Energy and Environment* 22 (2022): 29-39. https://doi.org/10.37934/progee.22.1.2939

[24] Huang, Kuan, Xi Feng, Xiao-Min Zhang, You-Ting Wu, and Xing-Bang Hu. "The ionic liquid-mediated Claus reaction: a highly efficient capture and conversion of hydrogen sulfide." *Green Chemistry* 18, no. 7 (2016): 1859-1863. https://doi.org/10.1039/C5GC03016A

[25] He, Yi, Jiang Yu, and Lingbo Chen. "Wet oxidation desulfurization of hydrogen sulfide with application of Fe-based ionic liquid." *CIESC J* 61, no. 4 (2010): 963-968.

[26] Li, Min, Jian Guan, Jing Han, Weizhao Liang, KunKun Wang, Erhong Duan, and Bin Guo. "Absorption and oxidation of H_2S in triethylamine hydrochloride· ferric chloride ionic liquids." *Journal of Molecular Liquids* 209 (2015): 58-61. https://doi.org/10.1016/j.molliq.2015.05.002

[27] Lo, Yi-Ting. "Synthesis and Characterization of Deep Eutectic Solvents (DES) with Multifunctional Building Blocks." *PhD diss., University of Akron*, 2019.

[28] Lin, Sui, Yang Fu, Luo Gen-Xiang, and Han Chun-Yu. "Hydrogen Sulfide Removal by Fe-Based Deep Eutectic Solvents." *Petroleum Processing and Petrochemicals* 46, no. 5 (2015): 23.

[29] Mutalib, Nor Fariza Abd, Mohamad Azmi Bustam, Mohd Dzul Hakim Wirzal, and Alamin Idris. "A Prediction for the Conversion Performance of H_2S to Elemental Sulfur in an Ionic-Liquid-Incorporated Transition Metal Using COSMO-RS." *Chemistry* 4, no. 3 (2022): 811-826. https://doi.org/10.3390/chemistry4030058

[30] Santos, E., J. Albo, and A. Irabien. "Magnetic ionic liquids: synthesis, properties and applications." *RSC Advances* 4, no. 75 (2014): 40008-40018. https://doi.org/10.1039/C4RA05156D

[31] Taheri, Mohsen, Ruisong Zhu, Gangqiang Yu, and Zhigang Lei. "Ionic liquid screening for CO_2 capture and H_2S removal from gases: The syngas purification case." *Chemical Engineering Science* 230 (2021): 116199. https://doi.org/10.1016/j.ces.2020.116199

[32] Balchandani, Sweta, and Ramesh Singh. "COSMO-RS Analysis of CO_2 Solubility in N-Methyldiethanolamine, Sulfolane, and 1-Butyl-3-methyl-imidazolium Acetate Activated by 2-Methylpiperazine for Postcombustion Carbon Capture." *ACS Omega* 6, no. 1 (2020): 747-761. https://doi.org/10.1021/acsomega.0c05298

[33] Salleh, M. Zulhaziman M., Mohamed K. Hadj-Kali, Mohd A. Hashim, and Sarwono Mulyono. "Ionic liquids for the separation of benzene and cyclohexane–COSMO-RS screening and experimental validation." *Journal of Molecular Liquids* 266 (2018): 51-61. https://doi.org/10.1016/j.molliq.2018.06.034

[34] Aki, Sudhir N. V. K, Berlyn R. Mellein, Eric M. Saurer, and Joan F. Brennecke. "High-pressure phase behavior of carbon dioxide with imidazolium-based ionic liquids." *The Journal of Physical Chemistry B* 108, no. 52 (2004): 20355-20365. https://doi.org/10.1021/jp046895

[35] Fredlake, Christopher P., Jacob M. Crosthwaite, Daniel G. Hert, Sudhir NVK Aki, and Joan F. Brennecke. "Thermophysical properties of imidazolium-based ionic liquids." *Journal of Chemical & Engineering Data* 49, no. 4 (2004): 954-964. https://doi.org/10.1021/je034261a

[36] Gu, Zhiyong, and Joan F. Brennecke. "Volume expansivities and isothermal compressibilities of imidazolium and pyridinium-based ionic liquids." *Journal of Chemical & Engineering Data* 47, no. 2 (2002): 339-345. https://doi.org/10.1021/je010242u

[37] Sakhaeinia, Hossein, Amir Hossein Jalili, Vahid Taghikhani, and Ali Akbar Safekordi. "Solubility of H_2S in Ionic Liquids 1-Ethyl-3-methylimidazolium Hexafluorophosphate ([emim][PF6]) and 1-Ethyl-3-methylimidazolium Bis (trifluoromethyl) sulfonylimide ([emim][Tf2N])." *Journal of Chemical & Engineering Data* 55, no. 12 (2010): 5839-5845. https://doi.org/10.1021/je100794k

[38] Santiago, Rubén, Jesus Lemus, Ana Xiao Outomuro, Jorge Bedia, and Jose Palomar. "Assessment of ionic liquids as H2S physical absorbents by thermodynamic and kinetic analysis based on process simulation." *Separation and Purification Technology* 233 (2020): 116050. https://doi.org/10.1016/j.seppur.2019.116050

[39] Zhong Ping, Tan, Wang Lin, and Wang Jian Bo. "Deprotection of t-butyldimethylsiloxy (TBDMS) protecting group with catalytic copper (II) chloride dihydrate." *Chinese Chemical Letters* 11, no. 9 (2000): 753-756.

[40] Maghsoodlu, M., Farzaneh Mohamadpour, Mojtaba Lashkari, and Nourallah Hazeri. "Convenient One-pot Access to Pyrano [2, 3-d] pyrimidine Derivatives via a CuCl2. 2H2O Catalyzed Knoevenagel-Michael Addition Reaction in Water/Ethanol Media." *Organic Chemistry Research* 4, no. 2 (2018): 140-146.

[41] Liu, Huiqing, Ruiyang Zhao, Xiuyan Song, Fusheng Liu, Shitao Yu, Shiwei Liu, and Xiaoping Ge. "Lewis acidic ionic liquid [Bmim] $FeCl_4$ as a high efficient catalyst for methanolysis of poly (lactic acid)." *Catalysis Letters* 147 (2017): 2298-2305. https://doi.org/10.1007/s10562-017-2138-x

[42] Ullah, Sami, Mohamad Azmi Bustam, Abdullah G. Al-Sehemi, Mohammed Ali Assiri, Girma Gonfa, Ahmad Mukhtar, Muhammad Ayoub, and Tausif Ahmad. "Experimental investigations on the regeneration of desulfurized 1-butyl-3-methylimidazolium tetrachloroferrate [Bmim][$FeCl_4$] and 1-butyl-3-methylimidazolium thiocyanate [Bmim][SCN] ionic liquids: A raman spectroscopic study." *Journal of Raman Spectroscopy* 51, no. 3 (2020): 546-554. https://doi.org/10.1002/jrs.5784